Astron. Astrophys. 334, L73–L76 (1998)

ASTRONOMY AND ASTROPHYSICS

LETTER

Letter to the Editor

The mid infrared spectrum of the hyperluminous galaxies IRAS F15307+3252 and the Cloverleaf⋆

H. Aussel[1], M. Gerin[2,3], F. Boulanger[4], F.X. Désert[5], F. Casoli[3], R.M. Cutri[6], and M. Signore[3]

[1] DAPNIA, Service d'Astrophysique, CEA/Saclay, Ormes des Merisiers, F-91191 Gif-sur-Yvette Cedex, France
[2] Radioastronomie, Ecole Normale Supérieure, 24 rue Lhomond, URA 336 du CNRS, F-75231 Paris Cedex 05, France
[3] DEMIRM, Observatoire de Paris, 61 avenue de l'Observatoire, URA 336 du CNRS, F-75014 Paris, France
[4] Institut d'Astrophysique Spatiale, Bât 121, Université Paris XI, F-91405 Orsay Cedex, France
[5] Observatoire de Grenoble, Domaine Universitaire, B.P. 53, F-38041 Grenoble Cedex 09, France
[6] IPAC, California Institute of Technology, MS 100-22, Pasadena, CA 91125, USA

Received 18 March 1998 / Accepted 21 April 1998

Abstract. We report the detections of the hyperluminous galaxy IRAS F15307 +3252 at $z = 0.93$ and of the Cloverleaf quasar, H 1413+117 at $z = 2.56$, in the mid infrared using ISOCAM. The spectrum near 10 μm (observed wavelength) joins smoothly with the data taken from the ground or with the IRAS satellite. We have detected none of the infrared features attributed to PAHs. For F15307 +3252, the mid-IR emission (9–16 μm observed wavelength) is 8×10^{45} erg s^{-1} ($q_0 = 0.5$, H$_0$ = 75 km s^{-1} Mpc^{-1}). This represents 10% of the total infrared emission from 5 to 200 μm (7.5×10^{46} erg s^{-1}). The shape of the mid-IR spectrum can be fitted by the emission of warm dust grains at a temperature of about 400 K. For the Cloverleaf QSO, H 1413+117, the grain temperature is even larger, $\simeq 1000K$. This intense near infrared emission can be used to put a lower limit on the size of the emitting regions of 5.7 pc for F15307 +3252 and $5/\sqrt{(m)}$ pc for the Cloverleaf where m is the magnification factor.

Key words: galaxies: active – ISM: dust – galaxies: individual: F15307 +3252 – galaxies: individual: H 1413+117

1. Introduction

After the discovery of the distant galaxy at $z = 2.3$ IRAS F10214+4724 in the IRAS data base (Rowan-Robinson et al. 1991), the search for similar objects led to the discovery of IRAS F15307 +3252 (Cutri et al. 1994) and to the recognition of an already known object as belonging to the same class: PG 09104+4109 (Kleinman et al. 1988, Taniguchi et al. 1997). There are now more than 20 objects known with IR luminosities larger than 10^{13} L$\odot$ (Rowan-Robinson 1995).

The Cloverleaf quasar (H 1413+117) at $z = 2.56$ was the first high redshift quasar to be detected in the submillimeter continuum and in carbon monoxyde emission (Barvainis et al. 1995). Its optical and radio images are split into four spots due to the presence of an intervening galaxy, yet unidentified, along the line of sight (Magain et al. 1988).

With a bolometric luminosity of 2×10^{13} $L_\odot$ (H_0 = 75 km s^{-1} Mpc^{-1}, $q_0 = 0.5$), F15307 +3252 is one of the most luminous galaxies known. Its optical and near-infrared spectrum resembles that of a Seyfert 2 galaxy (Cutri et al. 1994, Soifer et al. 1994) with a broad Hα emission line (Liu et al. 1996). K-band images obtained in good seeing with the Keck telescope show a complex morphology with multiple sources (Liu et al. 1996) which can be attributed either to an interacting system or to gravitational lensing. The K-band luminosity profile follows an $r^{1/4}$ law typical of elliptical galaxies and merger remnants. Hines et al. (1995) have found broad Mg II $\lambda 2798$ emission and a power law continuum in polarized light, which support the presence of a buried QSO. Adjusting the observed spectrum to a typical QSO spectrum, they deduce that the UV-optical continuum is dimmed by a factor 7–10, and infer an intrinsic UV-optical luminosity (1200 Å to 1 μm) of $L_{opt} \simeq 2 - 3 \times 10^{12} h^{-2} L_\odot$ for F15307 +3252. This value is typical of QSOs, and is sufficient to power 20% of the far-infrared emission from F15307 +3252. The scattering material responsible for the polarization is probably dust grains since the source has not been detected in X rays despite a very long integration time (Fabian et al. 1996). The gas column density must then be very high to block the X-rays radiation ($N_H \geq 10^{24}$ cm^{-2}).

Using ISOCAM on board ISO we have observed F15307 +3252 and the Cloverleaf quasar, and obtained their spectra betwen 5 and 16.5 μm and 9 and 16.5 μm respectively. We describe the observations in the next section and discuss the implications of our results in the last section.

Send offprint requests to: M. Gerin

⋆ Based on observations with the Infrared Space Observatory (ISO). ISO is an ESA project with instruments funded by ESA Member States (especially the PI countries: France, Germany, The Netherlands and the United Kingdom) and with participation of ISAS and NASA.

2. Observations

IRAS F15307 +3252 was observed by ISO with the camera ISOCAM (Cesarsky et al. 1996) using a circular variable filter (CVF) to sample the wavelength interval 5–16.5 μm with a pixel size of $6''$. Seven images of 10 seconds integration were recorded for each step of the CVF, for a total observing time of 11800 seconds. The spectral resolution of the CVF depends slightly on wavelength, and stays within the range 35 to 45. Because of higher redshift, the Cloverleaf was only observed from 9–16.5 μm, but using two wavelenghth scans, the first being performed downward, and the second upward. Six images with integration time of 5 seconds were recorded at each step, for a total integration time on the Cloverleaf is 4600 seconds.

The data for both sources were processed in six steps. The dark current of the camera is subtracted, then the readouts hit by cosmic rays are flagged. The ISOCAM transient behaviour is corrected using an inversion algorithm (Abergel et al. 1996) that has proven very efficient when dealing with CVF observations. The data are then flat-fielded to correct pixel to pixel gain variations. The dominant illumination source in the raw images is the zodiacal emission. Because of scattering within the camera, the zodiacal emission has wavelength dependent structures. We use two pieces of information to remove the zodiacal emission from the raw frames: (1) a 'running' sky image constructed by interpolating three calibration images taken on blank sky at 7.7, 11.4 and 15 μm; (2) a zodiacal spectrum obtained by averaging a large part of the images where no source is detected. The product of 'running' sky images and the zodiacal spectrum has been subtracted from the raw data. Finally, the ISOCAM images have been translated into physical units (mJy) using standard calibration files.

A point source is detected on the calibrated image at each wavelength, at the position of the target. In order to gain S/N ratio, we computed the spectrum of the source using only its brightest pixel. But the ISOCAM point spread function (PSF) extends over more than one pixel, and changes according to the wavelength. For example, for a source exactly centered on an ISOCAM pixel, this pixel will contain $\sim 70\%$ of the total flux of the source at 7μm but only $\sim 54\%$ at 15μm. We have corrected for this effect, using the ISOCAM PSF model developped by M. Pérault and K. Okumura, which has proven very accurate (Okumura 1997). The position of the source, relative to the camera pixel, has been measured with an accuracy of 0.6" (3σ), using a least square fit of the modelled PSF. The spectrum measured on the brightest pixel has been then corrected by the ratio of the flux falling into this pixel over the total flux, according to the model, thus maximizing the S/N. The final observed and rest-frame spectra are shown on Fig. 1. Although with the 6" pixel field of view the PSF is undersampled, the positioning of the source is not a dominant uncertainty factor on the photometry. The photometric accuracy is about 20%, an uncertainty related to the known gain variation from observation to observation. The detection of both sources with ISOCAM clearly confirms their identification with the IRAS sources. This point is particularly important for the source IRAS F15307 +3252, identified with a Seyfert 2 galaxy at $z = 0.93$ (Cutri et al. 1994), and which has not been detected yet at submillimeter and millimeter wavelengths. One additional source is present in the field of F15307 +3252, with a stellar spectrum. It is identified with the G0 star BD+33 2600 (SAO 64766) with a B magnitude of 9.7 mag.

3. Results

F15307+3252 is extremely faint between 5 and 8 μm with a flux density of about 3 mJy, but the flux increases rapidly to 10–20 mJy longward of 9 μm and joins smoothly the high value measured by the IRAS satellite at 25 μm (80 mJy). The 9.7 μm silicate feature falls at 18.7 μm in the observed frame, well beyond the passband of the CVF spectrum. The mid-IR spectrum from the Cloverleaf is also rising from 30 mJy at 9 μm to 40 mJy at 16 μm. The two spectra are remarkably featureless with no hint of the infrared features due to PAHs. For F15307 +3252, the 6.2, 7.7 and 8.6 μm features fall within the observed spectral passband. These bands are seen in nearby galaxies at large contrast to the underlying continuum: about 4 for the 6.2 μm feature in the starburst galaxy NGC 6090 (Acosta-Pulido et al. 1996), $\sim$ 50–100% in the active galaxy Circinus (Moorwood et al. 1996), but they are absent towards the nucleus of NGC 1068 (Lutzet al. 1996). Toward F15307 +3252, the spectrum near 12 μm, where the 6.2 μm feature is expected to show up, is clean. With a peak to peak noise level of 6 mJy, the maximum contrast for this feature is 40%. There are two weak bumps at 14.5 and 15.7 μm, close to the expected positions of the 7.7 and 8.6 μm features (14.8 and 16.6 μm). However, because only a single spectral scan was obtained, it is impossible to rule out that these are spurious features caused by memory effects after glitches. The upper limit to the contrast of these features is $\sim$ 30%. For the Cloverleaf, we would have expected to see the 3.3 μm feature. Again, the maximum contrast is 20%.

4. Discussion

4.1. Dust temperature and size of the emitting region

We show on Fig. 2 the spectral energy distribution (SED) of the Cloverleaf and IRAS F15307 +3252, calculated as νL_ν, from far infrared to visible wavelengths in the rest frame of these galaxies. For the Cloverleaf, the SED shape shows that there is a wide distribution of dust temperatures down to 100 K. The cold component of the dust is associated with the CO emission (Kneib et al. 1998), which size has been estimated to be 200 pc by Yun et al. (1997). The mid infrared part comes from warmer grains; it is well fitted by a $\sim 1000K$ dust with a λ^{-1} emissivity. This temperature is better constrained in F15307 +3252 where the steep increase of the emission in the mid-IR implies a dust temperature of 400 ± 50 K with again an emissivity scaling as λ^{-1}.

These temperature estimates can be used to infer the size of the emitting region. With a λ^{-1} emissivity, the equilibrium dust temperature is related to the distance to the illuminating source by the equation (Sanders et al. 1989) $T \sim 1200 L_{46}^{1/5} r_{pc}^{-2/5}$

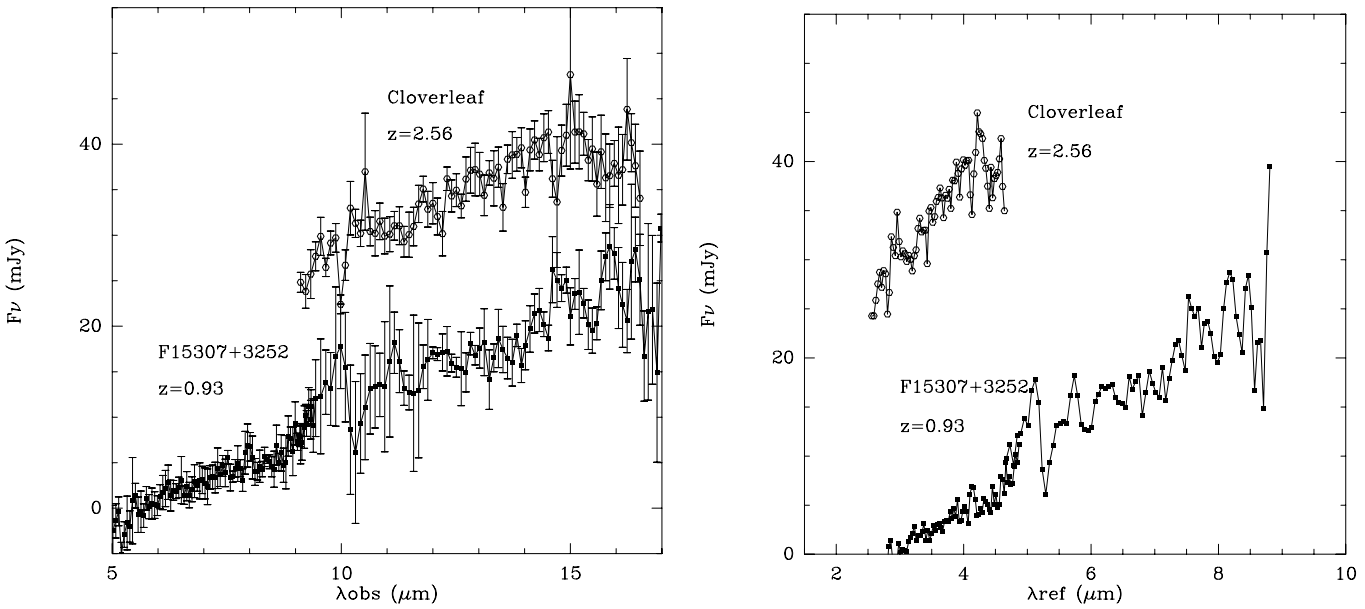

a Observed spectra

b Rest frame spectra

Fig. 1a and b. ISOCAM observed and rest frame spectra of the Cloverleaf and IRAS F15307+3252 between 5 and 16.5 μm. Towards F15307+3252, the spectrum is noiser between 10 and 12 μm (observed wavelength) due to impact by cosmic rays.

where L_{46} is the luminosity of the central source in units of 10^{46} erg/s and r_{pc} the distance to the source in parsecs. For both sources, we assume that the bolometric luminosity comes mainly from the nucleus.If the dust grains are large enough to be in equilibrium with the radiation field, we derive for F15307 +3252 a distance from the central nucleus to the dust source of 41 pc, given the total bolometric luminosity of $\sim 7 \times 10^{46}$ erg/s (H_0 = 75 km s^{-1} Mpc^{-1}, $q_0 = 0.5$). For the Cloverleaf, the result depends on the magnification factor m. With a bolometric luminosity of $3 \times 10^{47}/m$, we find a size of $8/\sqrt{(}m)$ pc.

A lower limit on the size of the emitting region can be set assuming that the source emits as a black body at mid infrared wavelengths. The 9–16 μm (observed wavelength) luminosities of the Cloverleaf and F15307 +3252 are respectively $1.7/m \times 10^{47}$ erg/s and 8.8×10^{45} erg/s. The derived source sizes are $5/\sqrt{(}m)$ pc and 5.7 pc for the Cloverleaf and F15307+3252 respectively.

A unified model of active galactic nuclei (AGN) has been proposed to account for observations of Seyfert 1 and 2 galaxies, based on a dust torus which inclination determines the extinction of the X-ray and UV emission. Various authors have calculated the infrared emission of this torus. In this framework, the mid-IR radiation is produces from the warmest dust grains, located at the inner radius of the torus. Specific models for F15307 +3252 and the Cloverleaf are presented by Granato et al. (1996). The difference in the shape of the SEDs between the Cloverleaf and F15307 +3252 could correspond to a difference of viewing angle of the dust torus: almost face-on for the Cloverleaf and close to edge-on for F15307 +3252 (Granato et al. 1996). Our measurements of the IR emission allows to constrain better this model, due to the better determination of the dust temperature.

4.2. Detectability of PAHs features

Apart from probing the hot dust content, the mid-IR emission allows to possibly test the presence of the carrier of Unidentified Infrared Bands (UIB) in a hard spectrum environment. Désert and Dennefeld (1988) compared the strength of the PAHs features with the Spectral Energy Distribution (SED) in starburst and active galaxies. At small scale (0.1–1 kpc) the features weaken or disappear in the vicinity of active nuclei. Indeed, many author have presented models where these carriers, identified as PAHs, should be destroyed by the hard radiation from the central source. Voit (1992) has shown that soft X-rays can easily destroy PAHs even at large distance (up to 1 kpc) from an active nucleus. ISO observations of Galactic HII regions and galaxies provide evidence for evolution of the strength and shape of the IR features, in very strong UV fields ($G_0 \gtrsim 10^5$, Cesarsky et al. 1996, Vigroux 1998). At these energy densities, the spectrum which shows only faint dust features, is dominated by the continuum emission from small grains rather than PAHs. This probably implies that PAHs are destroyed, although it has not yet been quantified.

The featureless IR emission due to the warm dust grains ($T \sim 400K$), associated with the inner region of the dust torus is so strong in F 15307+3252, that it could hide the emission in the PAHs features. In photon dominated regions (PDRs), the fraction of the dust emission in the PAHs features is $\sim 18\%$ (Boulanger et al. 1996). If the larger grains are warm enough to emit in the same wavelength range than PAHs, the PAHs emission will have a weak contrast. The signal to noise in the data is not good enough to detect the bands, if their contrast with respect to continuum emission is the same as in the M17 HII

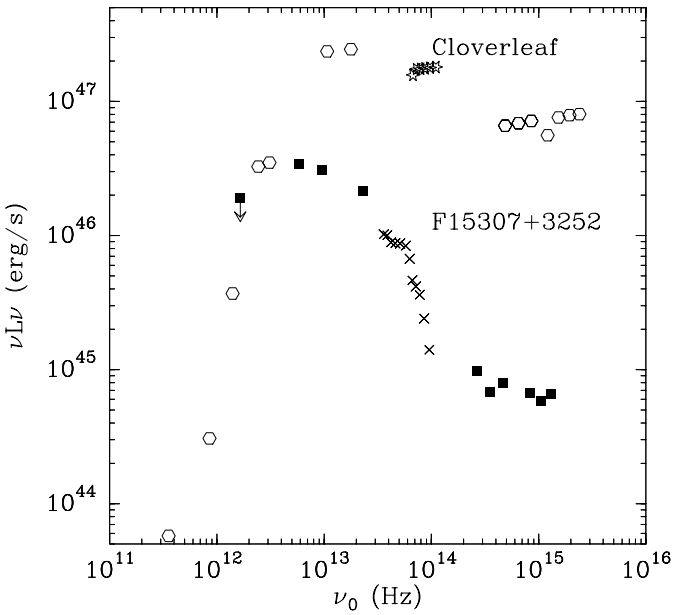

Fig. 2. Spectral energy distribution of the Cloverleaf (hexagons and stars) and IRAS F15307 +3252 (black squares and crosses) from visible to far infrared wavelengths, given as νL_ν in the rest frame of these objects. Distances have been calculated using H_0 = 75 km s^{-1} Mpc^{-1} and $q_0 = 0.5$. Data for the Cloverleaf are taken from Barvainis et al. (1995); For F15307+5252, we used data from Cutri et al. (1994), Hines et al. (1995) and Lis (private communication). The ISOCAM data ar with stars and crosses for the Cloverleaf and F15307 +3252 respectively.

region. We cannot therefore decide if the PAHs are destroyed in the inner part of the dust torus. In the outer part, there will not be enough radiation to make a significant contribution to the mid infrared emission. For the Cloverleaf, the detection of the 3.3 μm feature is even more difficult because the energy radiated in this feature is less than 1% of the total dust emission.

For both objects, the nucleus is so bright that it is hard to detect emission from a possible starburst in the host galaxy. For example, in NGC 6090, the emission in the PAHs features is 10^{10} $L_\odot$ (Acosta-Pulido et al. 1996), which represents 10% of the total IR luminosity of this galaxy (10^{11} $L_\odot$). For F15307 +3252, the 9–16 μm luminosity is 2×10^{12} $L_\odot$. The emission in the PAHs features from a starburst similar to NGC 6090 therefore represents 0.5% only of the luminosity of F15307 +3252 in this wavelength range. A signal to noise ratio in the continuum ≥ 200 would be required to detect features in F15307 +3252 having the same luminosity as in NGC 6090. This is much higher than that achieved in our ISO measurements.

Acknowledgements. We thank D. Lutz for the communication of the SWS spectrum of NGC 1068, and D. Lis for observing F15307 +3252 at the Caltech Submillimeter Observatory. We made use of the CAM Interactive Analysis Software (CIA), a joint development by the ESA Astrophysics Division and the ISOCAM Consortium led by the ISOCAM PI, C. Cesarsky, Direction des Sciences de la Matière, C.E.A., France. RMC acknowledges the support of the Jet Propulsion Laboratory, Caltech, which is operated under contract with NASA.

References

Abergel A. et al., 1996, A&A 315, L329
Acosta-Pulido J.A., Klaas U., Laureijs R.J., et al., 1996, A&A 315, L121.
Barvainis R., Antonucci R., Hurt T., Coleman P., Reuter H.P., 1995, ApJ 451, L9.
Boulanger F., Reach W.T., Abergel A. et al. 1996, A&A 315, L325.
Cesarsky C.J., Abergel A., Agnèse P. et al. 1996, A&A 315, L32.
Cesarsky D., Lequeux J., Abergel A. et al., A&A 315, 309
Cutri R.M., Huchra J.P., Low F.J., Brown R.L., Vanden Bout P. A., 1994, ApJ 424, L65.
Désert F.X., Dennefeld M., 1988, A&A 206, 227.
Fabian A.C., Cutri R.M., Smith H.E., Crawford C.S., Brandt W.N., 1996, MNRAS 283, L95.
Granato G.L., Danese L., Franceschini A., 1996, ApJ 460 L11.
Hines D.C., Schmidt G.D., Smith P.S., Cutri R.M., Low F.J., 1995, ApJ 450, L1.
Kleinman S.G., Hamilton D., Keel W.C. et al., 1988, ApJ 328, 161.
Kneib J.P., Alloin D., Mellier Y. et al., 1998, A&A 329, 827.
Liu M.C., Graham J.R., Wright G.S., 1996, ApJ 470, 771.
Lutz D., Sturm E., Genzel R., Moorwood A.F.M., Sternberg A., 1997, Astrophys. space Science 248, 217.
Magain P., Surdej J., Condon J.J., et al., 1988, Nature 334, 325.
Moorwood A.M., Lutz D., Oliva E. et al., 1996, A&A 315, L109.
Okumura K., 1997, CAM PSF report, *http://isowww.estec.esa.nl:80/instr/CAM/cal_wksp/*
Rowan-Robinson M. et al. 1991, Nature 351, 719.
Rowan-Robinson M., 1995, in "Cold gas at high redshift" p 61.
Sanders D.B., Phinney E.S., Neugebauer G., Soifer B.T., Matthews K., 1989, ApJ 347, 29.
Soifer B.T., Neugebauer G., Matthews K., Armus L., 1994, ApJ 433, L69.
Taniguchi Y., Sato Y., Kawara K., Mirayama T., Mouri H., 1997, A&A 318, L1.
Verstraete L., Puget J.L., Falgarone E., et al., 1996, A&A 315, L337.
Vigroux L., 1998, in "Extragalactic astronomy in the infrared", G.A. Mamon, T.X. Thuan and J. T. T. Van eds, p 63.
Voit G.M., 1992, MNRAS 258, 841.
Yun M.S., Scoville N. Z., Carrasco J.J., Blandford R.D., 1997, ApJ 479, L9.